

An element-based 9-node resultant shell element for large deformation analysis of laminated composite plates and shells

S. C. Han[†]

Department of Civil Engineering, Daewon Science College, Jecheon, Chung-Buk 390-702, Korea

K. D. Kim[†] and W. Kanok-Nukulchai[‡]

School of Civil Engineering, Asian Institute of Technology, Klongluang, Pathumthani, 12120, Thailand

(Received November 15, 2003, Accepted October 3, 2004)

Abstract. The Element-Based Lagrangian Formulation of a 9-node resultant-stress shell element is presented for the isotropic and anisotropic composite material. The effect of the coupling term between the bending strain and displacement has been investigated in the warping problem. The strains, stresses and constitutive equations based on the natural co-ordinate have been used throughout the Element-Based Lagrangian Formulation of the present shell element which offers an advantage of easy implementation compared with the traditional Lagrangian Formulation. The element is free of both membrane and shear locking behavior by using the assumed natural strain method such that the element performs very well in thin shell problems. In composite plates and shells, the transverse shear stiffness is defined by an equilibrium approach instead of using the shear correction factor. The arc-length control method is used to trace complex equilibrium paths in thin shell applications. Several numerical analyses are presented and discussed in order to investigate the capabilities of the present shell element. The results showed very good agreement compared with well-established formulations in the literature.

Key words: 9-node resultant shell element; Element-based Lagrangian Formulation; laminated composite plates and shells; assumed strain method; arc-length control method.

1. Introduction

In recent years, fibre-reinforced composite materials a new class of materials, have increasingly being used in a large variety of structures including aerospace, marine and civil infrastructure fields. Composite structures offer an attractive alternative to more conventional forms of construction due to its high strength to weight ratio and resistance to corrosion. Recently, there has been a major emphasis made on the use of FRP composite materials as a means of developing new high performance alternative materials for infrastructure applications such as seismic column wrapping and lightweight deck development.

[†] Associate Professor

[‡] Professor

The modeling of shell structures represents a challenging task since the early developments of the finite element method. In fact, papers on the subject (focusing on computational aspects) can be traced back to the original work of Ahmad *et al.* (1970). This work represented the onset of the so-called degenerated approach, with a three-dimensional continuum being modeled by means of a reference surface. Following this concept, isoparametric finite elements were formulated using independent rotational and displacements degrees of freedom. Further, normal stresses in the direction of the shell thickness were not included in the formulation. The original concept was then extended to the non-linear range in the works of Ramm (1977), Hughes and Liu (1981) and Liu *et al.* (1986), among many others.

However, a defect of this class of elements was found when thin shells were analyzed. Huang and Hinton (1986) developed a 9 node assumed strain shell element. They used an enhanced interpolation of the transverse shear strains in the natural coordinate system to overcome the shear locking problems. Other finite elements employing the assumed strain method were then reported by Jang and Pinsky (1987) independently and also a variational background of the assumed strain method was presented by Simo and Hughes (1986). Belytschko *et al.* (1989) presented a 9-node assumed strain shell element with a stabilized matrix to control the hourglass modes. All the terms in this shell element used a reduced integration.

Of these elements, for purpose of computational efficiency, the 'resultant-stress' theories may be used, wherein the generalized stresses are the membrane forces, shear forces and moments, respectively. The major drawback has arisen in the implementation of this method. Some developments of the strain-displacement matrices from degenerated shell theory lead to the isotropic and laminated composite elements that fail in problems such as twisted shells.

In large deformation analysis, the linearized non-linear equation has to be derived in order to solve the non-linear equations of the structural system via Lagrangian formulations. Kanok-Nukulchai and Wong (1988) introduced a new Lagrangian formulation referred to as the Element-Based Lagrangian Formulation (ELF) since the parental element serves as a deformation reference in ELF. It means that all equations governing a deformed body can be expressed with respect to natural coordinate systems and so it appears in a simpler form than those of the traditional Lagrangian approaches. Lee and Kanok-Nukulchai (1998) presented a 9-node shell element using an Element-Based Lagrangian Formulation concept for large deformation analysis of shell structures. The Element-Based Lagrangian Formulation makes implementation simpler and easier than the traditional Lagrangian formulations, especially when the assumed natural strain method is involved. The shell element is based on the resultant-stress theories with the transverse shear deformation. By using the assumed strain methods, the shell element is free of the membrane and shear locking in the thin shell limit. All the results have very good agreement with references. However, the coupling terms between the bending strain and displacement are ignored in the curvature. These terms are particularly important in the twisted shell problem, where their absence leads to severe errors.

However, the development of laminated shell elements for large deformation analysis has been less attempted, than those of single layered isotropic shell elements. In order to develop a laminated shell element for large deformation analysis, a very similar development procedure to that of the single layered shell elements is needed. However, the equivalent constitutive equation should be utilized for the computationally efficient composite element. The resultant shell element concept used an equivalent constitutive equation model which obtains the constitutive law of the equivalent medium in terms of the properties of the individual layers. This concept was extended to the linear and non-linear range in the 8-node finite element works of Kim *et al.* (1998), Kim and Voyiadjis (1999), and

Kim and Park (2002). In order to improve the transverse shear stiffness, Rolfes and Rohwer (1997) assumed two cylindrical bending modes for an improved transverse shear modulus based on first order shear deformation theory for finite elements. In this study, equivalent natural constitutive equation is derived using an explicit transformation scheme to capture the multi-layer effect.

The objective of this paper is to present the formulation of a geometrically nonlinear 9-node shell element based on the resultant-stress formulation and its application to geometrical nonlinear analysis of laminate composite shell structures. The ELF concept is adopted to present the initial configuration and deformed configurations of the present finite element. The assumed natural strain method has been used to remove the locking problems by the ELF form. In the laminated composite formulation, instead of using the conventional transverse shear correction factor for laminates, the equilibrium approach suggested by Rolfes and Rowher (1997) is used.

The formulation of the resultant shell element is based on Mindlin-Reissner theory, assuming small strains and large rotations. The geometric stiffness is analytically integrated through the thickness. In comparison with volume integration, which is generally used in the degenerated shell elements, the computational time is significantly reduced for geometrically nonlinear analysis of laminated composite structures. The effect of coupling term between the bending and membrane strain-displacement matrix is investigated in the twisted beam problem. The results showed the improvement caused by the coupling term in this example.

2. Geometry and kinematics of the shell element

Generally the Lagrangian formulations for geometric nonlinear case can be classified into two approaches: namely, (1) Total Lagrangian Formulation (TLF), where all the static and kinematic

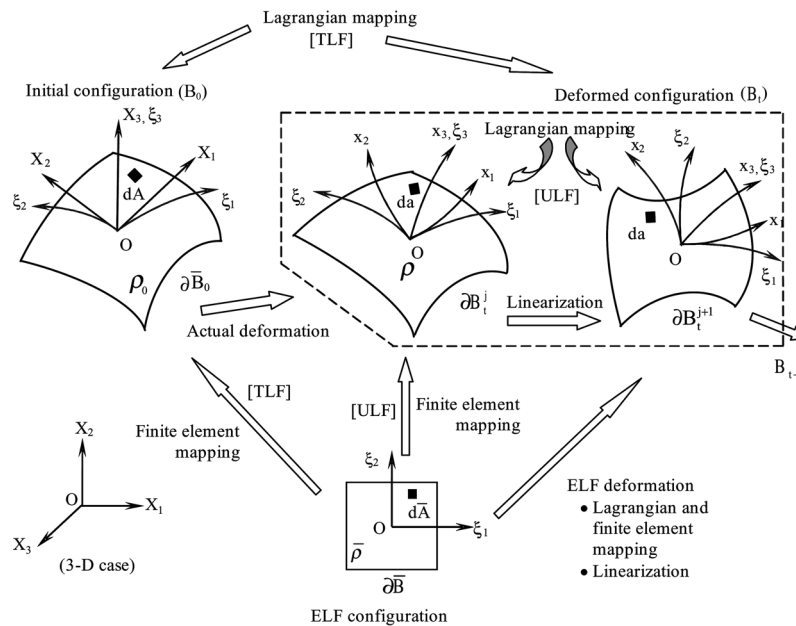


Fig. 1 The Element-Based Lagrangian Formulation method

variables are referred back to the initial undeformed configuration (\mathbf{B}_0), (2) Updated Lagrangian Formulation (ULF), where all are referred to the current deformed configuration (\mathbf{B}_t).

Wong (1984) has proposed a new variation of Lagrangian formulation known as Element-based Lagrangian Formulation (ELF), where all the static and kinematic variables are referred to a nonphysical “Element-based” configuration ($\bar{\mathbf{B}}$) as shown in Fig. 1. Unlike the two traditional Lagrangian formulations, a standard parental element serving as the reference of deformation is to be mapped directly into each element of the initial and deformed configurations in the Element-based Lagrangian Formulation. Therefore, all balance equations governing the deformed configuration can be expressed over the parental element domain in terms of the element natural co-ordinates. It should be noted that these three approaches for a problem should theoretically yield the same result.

The geometry of 9-node shell element shown is Fig. 2 has six degrees of freedom per node. The initial geometry of the nine-node Lagrangian element shown in Fig. 3 is defined by the following

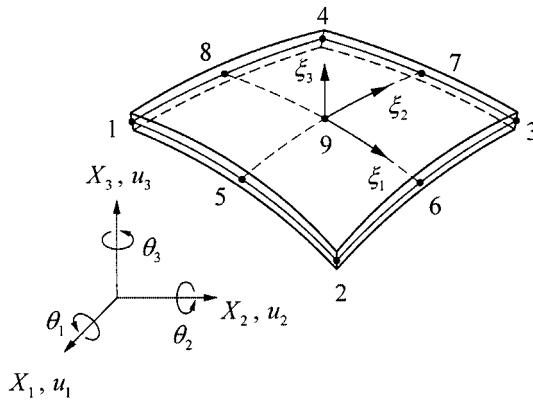


Fig. 2 Geometry of 9-node shell element with six degrees of freedom

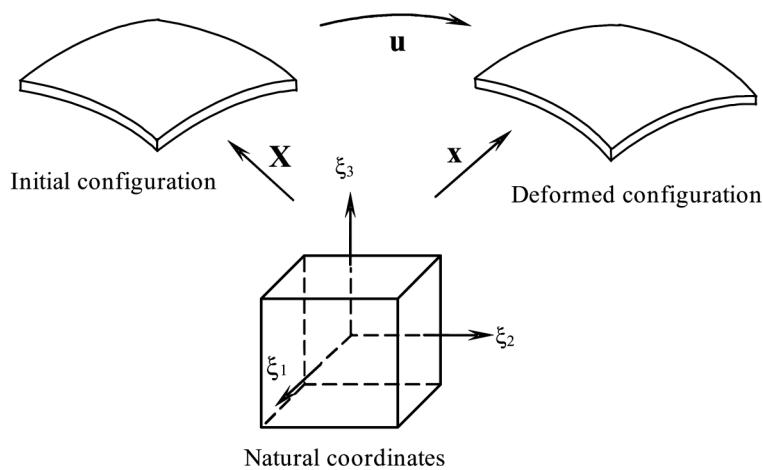


Fig. 3 Initial and deformed geometries of a shell element

relations. The initial configuration of the shell element having constant thickness h can be written as

$$\mathbf{X}(\xi_1, \xi_2, \xi_3) = \bar{\mathbf{X}}(\xi_1, \xi_2) + \mathbf{D}(\xi_1, \xi_2, \xi_3) \quad (1)$$

where

$$\begin{aligned} \bar{\mathbf{X}}(\xi_1, \xi_2) &= \sum_{a=1}^9 N^a(\xi_1, \xi_2) \bar{\mathbf{X}}^a \\ \mathbf{D}(\xi_1, \xi_2, \xi_3) &= \sum_{a=1}^9 N^a(\xi_1, \xi_2) \mathbf{D}^a \\ \mathbf{D}^a(\xi_3) &= \frac{h^a \xi_3}{2} \hat{\mathbf{D}}^a \end{aligned} \quad (2)$$

where $\bar{\mathbf{X}}^a$ are position vectors which have three Cartesian components, \mathbf{D}^a are nine unit normal vectors and $\hat{\mathbf{D}}^a$ is a unit normal vector at node a .

The following relations are introduced for the definition of deformed geometry of the element.

$$\mathbf{x}(\xi_1, \xi_2, \xi_3) = \sum_{a=1}^9 N^a(\xi_1, \xi_2) \left[\bar{\mathbf{x}}^a + \frac{\xi_3 h^a}{2} \hat{\mathbf{d}}^a \right] = \bar{\mathbf{x}} + \xi_3 \bar{\mathbf{d}} \quad (3)$$

In Eq. (3), \mathbf{x} , $\bar{\mathbf{x}}$, $\bar{\mathbf{d}}$, $\bar{\mathbf{x}}_a$, \mathbf{d}^a and $\hat{\mathbf{d}}^a$ in the deformed geometry correspond to \mathbf{X} , $\bar{\mathbf{X}}$, $\bar{\mathbf{D}}$, $\bar{\mathbf{X}}^a$, \mathbf{D}^a and $\hat{\mathbf{D}}^a$ in Eqs. (1)-(2). Hence, the displacement field \mathbf{u} in the shell element can be defined as

$$\mathbf{u}(\xi_1, \xi_2, \xi_3) = \sum_{a=1}^9 N^a(\xi_1, \xi_2) \left[\bar{\mathbf{u}}^a + \frac{\xi_3 h^a}{2} \hat{\mathbf{e}}^a \right] = \bar{\mathbf{u}} + \xi_3 \bar{\mathbf{e}} \quad (4)$$

where, at the node a the translational displacement vector $\bar{\mathbf{u}}^a = \bar{\mathbf{x}}^a - \bar{\mathbf{X}}^a$, and the fibre displacement vector $\hat{\mathbf{e}}^a = \hat{\mathbf{d}}^a - \hat{\mathbf{D}}^a$.

The translational displacement field can be expressed by shape functions in terms of nodal translational as shown in the first part of the right-hand side of Eq. (4). The three successive rotations θ_1 , θ_2 and θ_3 have been introduced to express finite rotational displacement instead of the Euler angle which usually guarantees the independence of two rotations in the Lagrangian formulation since six degrees of freedom are adopted in the present study. If we introduce another set of Cartesian co-ordinates at the nodal points with the assumption that the unit normal vectors are firmly fixed into it and they move with the body, rotations which are undergone by the unit normal vector during deformation could be expressed elegantly via this co-ordinate set.

Basically, the transformation matrices for these rotations are

$$T_{R1}(\theta_1) = \begin{bmatrix} 1 & 0 & 0 \\ 0 & \cos \theta_1 & -\sin \theta_1 \\ 0 & \sin \theta_1 & \cos \theta_1 \end{bmatrix}; \quad T_{R2}(\theta_2) = \begin{bmatrix} \cos \theta_2 & 0 & \sin \theta_2 \\ 0 & 1 & 0 \\ -\sin \theta_2 & 0 & \cos \theta_2 \end{bmatrix}; \quad T_{R3}(\theta_3) = \begin{bmatrix} \cos \theta_3 & -\sin \theta_3 & 0 \\ \sin \theta_3 & \cos \theta_3 & 0 \\ 0 & 0 & 1 \end{bmatrix} \quad (5)$$

However, it is important to note that three successive rotations used in this study lost their vectorial characteristics which remained in the cases when the rotations were infinitesimal. After undergoing three rotations successively, the transformation matrix between the initial shell normal and the deformed normal can be written as the result of a sequence of finite rotations θ_1 , θ_2 and θ_3 as follows;

$$\begin{aligned} \mathbf{T}_R &= T_{R1}(\theta_1)T_{R2}(\theta_2)T_{R3}(\theta_3) \\ &= \begin{bmatrix} \cos\theta_2\cos\theta_3 & -\cos\theta_2\sin\theta_3 & \sin\theta_2 \\ \cos\theta_1\sin\theta_3 + \sin\theta_1\sin\theta_2\cos\theta_3 & \cos\theta_1\cos\theta_3 - \sin\theta_1\sin\theta_2\sin\theta_3 & -\sin\theta_1\cos\theta_2 \\ \sin\theta_1\sin\theta_3 - \cos\theta_1\sin\theta_2\cos\theta_3 & \sin\theta_1\cos\theta_3 + \cos\theta_1\sin\theta_2\sin\theta_3 & \cos\theta_1\cos\theta_2 \end{bmatrix} \end{aligned} \quad (6)$$

Consequently, using the transformation matrix of Eq. (6), the displacement field in Eq. (4) can be expressed as

$$\mathbf{u}(\xi_1, \xi_2, \xi_3) = \sum_{a=1}^9 N^a(\xi_1, \xi_2) \left[\bar{\mathbf{u}}^a + \frac{\xi_3 h^a}{2} (\mathbf{T}_R^a - \mathbf{I}_{3 \times 3}) \hat{\mathbf{D}}^a \right] \quad (7)$$

where $\mathbf{I}_{3 \times 3}$ is a unit matrix.

In addition, with some mathematical manipulation, the incremental form of the displacement field for the present shell element may be written in terms of the nodal incremental vector $\Delta \mathbf{U}^a$ as

$$\Delta \mathbf{u}(\xi_1, \xi_2, \xi_3) = \sum_{a=1}^9 N^a(\xi_1, \xi_2) [\mathbf{I}_{3 \times 3} | \xi_3 \mathbf{V}^a] \Delta \mathbf{U}^a \quad (8)$$

where

$$\mathbf{V}^a = \frac{h^a}{2} \mathbf{T}_R^a \Phi^a \mathbf{T}_A, \quad \Delta \mathbf{U}^a = \{\Delta \bar{u}_1^a, \Delta \bar{u}_2^a, \Delta \bar{u}_3^a, \Delta \theta_1^a, \Delta \theta_2^a, \Delta \theta_3^a\} \quad (9)$$

in which

$$\Phi^a = \begin{bmatrix} 0 & \hat{D}_3^a & -\hat{D}_2^a \\ -\hat{D}_3^a & 0 & \hat{D}_1^a \\ \hat{D}_2^a & -\hat{D}_1^a & 0 \end{bmatrix}; \quad \mathbf{T}_A = \begin{bmatrix} \cos\theta_2\cos\theta_3 & \sin\theta_3 & 0 \\ -\cos\theta_2\sin\theta_3 & \cos\theta_3 & 0 \\ \sin\theta_2 & 0 & 1 \end{bmatrix} \quad (10-1,2)$$

3. Natural strain tensor

In the Element-based Lagrangian formulation, an Element-based strain tensor will be defined with respect to the convected curvilinear coordinates (ξ_1, ξ_2, ξ_3) as

$$\tilde{E}_{\alpha\beta} = \frac{1}{2}(g_{\alpha\beta} - G_{\alpha\beta}) \quad (11)$$

in which $g_{\alpha\beta}$ and $G_{\alpha\beta}$ are the covariant components of the metric tensors to be obtained from the basis vector $g_\alpha = \frac{\partial x_i}{\partial \xi_\alpha} \mathbf{I}_i$ and $G_\beta = \frac{\partial X_I}{\partial \xi_\beta} \mathbf{I}_I$ which are tangents to the curvilinear coordinate lines in \mathbf{B}_t and \mathbf{B}_0 respectively, i.e.,

$$g_{\alpha\beta} = g_\alpha \cdot g_\beta = \frac{\partial x_i}{\partial \xi_\alpha} \frac{\partial x_i}{\partial \xi_\beta}, \quad G_{\alpha\beta} = G_\alpha \cdot G_\beta = \frac{\partial X_I}{\partial \xi_\alpha} \frac{\partial X_I}{\partial \xi_\beta} \quad (12)$$

Two major different definitions of strain, the so-called Lagrangian strain and the Eulerian strain, which depend on the reference system measuring the deformation, have been extensively used in the formulation of large deformation analysis. However, since the formulation used in this study refers to the natural reference system, following the element-based Lagrangian formulation (Kanok-Nukulchai and Wong 1988), the natural strain tensor corresponding to the Green strain tensor may be defined as

$$\tilde{E}_{\alpha\beta} = \frac{1}{2} \left(\frac{\partial x_i}{\partial \xi_\alpha} \frac{\partial x_i}{\partial \xi_\beta} - \frac{\partial X_I}{\partial \xi_\alpha} \frac{\partial X_I}{\partial \xi_\beta} \right) \quad (13)$$

It should be noted that the Green strain tensor and the natural strain have the following tensor transformation relationship.

$$\begin{aligned} \tilde{E}_{\alpha\beta} &= \frac{\partial X_I}{\partial \xi_\alpha} \frac{\partial X_J}{\partial \xi_\beta} E_{IJ} \\ &= \frac{1}{2} \left[\frac{\partial X_I}{\partial \xi_\alpha} \frac{\partial u_I}{\partial \xi_\beta} + \frac{\partial u_J}{\partial \xi_\alpha} \frac{\partial X_J}{\partial \xi_\beta} + \frac{\partial u_K}{\partial \xi_\alpha} \frac{\partial u_K}{\partial \xi_\beta} \right] \end{aligned} \quad (14)$$

By substituting Eq. (1) and Eq. (4) in Eq. (14), and using a shifter transformation between the local and global displacement, the following strain-displacement relation can be obtained

$$\tilde{E}_{\alpha\beta} = \frac{1}{2} \left[\frac{\partial(\bar{X}_I + \xi_3 \bar{D}_I)}{\partial \xi_\alpha} \frac{\partial(\bar{u}_I + \xi_3 \bar{e}_I)}{\partial \xi_\beta} + \frac{\partial(\bar{u}_J + \xi_3 \bar{e}_J)}{\partial \xi_\alpha} \frac{\partial(\bar{X}_J + \xi_3 \bar{D}_J)}{\partial \xi_\beta} + \frac{\partial(\bar{u}_K + \xi_3 \bar{e}_K)}{\partial \xi_\alpha} \frac{\partial(\bar{u}_K + \xi_3 \bar{e}_K)}{\partial \xi_\beta} \right] \quad (15)$$

The incremental membrane, bending and transverse shear strains with Eq. (9) can be separated into linear and nonlinear parts such as:

$$\begin{aligned} \Delta \tilde{E}^m &= \Delta^L \tilde{E}^m + \Delta^{NL} \tilde{E}^m \\ \Delta \tilde{E}^b &= \Delta^L \tilde{E}^b + \Delta^{NL} \tilde{E}^b \\ \Delta \tilde{E}^s &= \Delta^L \tilde{E}^s + \Delta^{NL} \tilde{E}^s \end{aligned} \quad (16)$$

where

$$\Delta^L \tilde{E}^m = \begin{bmatrix} \frac{\partial \bar{X}_1}{\partial \xi_1} \frac{\partial}{\partial \xi_1} & 0 & 0 \\ 0 & \frac{\partial \bar{X}_2}{\partial \xi_2} \frac{\partial}{\partial \xi_2} & 0 \\ \frac{1}{2} \left(\frac{\partial \bar{X}_1}{\partial \xi_1} \frac{\partial}{\partial \xi_2} \right) & \frac{1}{2} \left(\frac{\partial \bar{X}_2}{\partial \xi_2} \frac{\partial}{\partial \xi_1} \right) & 0 \end{bmatrix} \begin{Bmatrix} \Delta \bar{u}_1 \\ \Delta \bar{u}_2 \\ \Delta \bar{u}_3 \end{Bmatrix} = \tilde{\mathbf{B}}_m \Delta \bar{u} \quad (17)$$

$$\Delta^L \tilde{E}^b = \xi_3 \begin{bmatrix} \frac{\partial \bar{D}_1}{\partial \xi_1} \frac{\partial}{\partial \xi_1} & 0 & 0 & \frac{\partial \bar{X}_1}{\partial \xi_1} \frac{\partial}{\partial \xi_1} & 0 & 0 \\ 0 & \frac{\partial \bar{D}_2}{\partial \xi_2} \frac{\partial}{\partial \xi_2} & 0 & 0 & \frac{\partial \bar{X}_2}{\partial \xi_2} \frac{\partial}{\partial \xi_2} & 0 \\ \frac{1}{2} \left(\frac{\partial \bar{D}_1}{\partial \xi_1} \frac{\partial}{\partial \xi_2} \right) & \frac{1}{2} \left(\frac{\partial \bar{D}_2}{\partial \xi_2} \frac{\partial}{\partial \xi_1} \right) & 0 & \frac{1}{2} \left(\frac{\partial \bar{X}_1}{\partial \xi_1} \frac{\partial}{\partial \xi_2} \right) & \frac{1}{2} \left(\frac{\partial \bar{X}_2}{\partial \xi_2} \frac{\partial}{\partial \xi_1} \right) & 0 \end{bmatrix} \begin{Bmatrix} \Delta \bar{u}_1 \\ \Delta \bar{u}_2 \\ \Delta \bar{u}_3 \\ \Delta \bar{e}_1 \\ \Delta \bar{e}_2 \\ \Delta \bar{e}_3 \end{Bmatrix} = \xi_3 \tilde{\mathbf{B}}_b \Delta \mathbf{U} \quad (18)$$

$$\Delta^L \tilde{E}^s = \begin{bmatrix} 0 & 0 & \frac{1}{2} \left(\bar{D}_3 \frac{\partial}{\partial \xi_2} \right) & 0 & \frac{1}{2} \frac{\partial \bar{X}_2}{\partial \xi_2} & 0 \\ 0 & 0 & \frac{1}{2} \left(\bar{D}_3 \frac{\partial}{\partial \xi_1} \right) & \frac{1}{2} \frac{\partial \bar{X}_1}{\partial \xi_1} & 0 & 0 \end{bmatrix} \begin{Bmatrix} \Delta \bar{u}_1 \\ \Delta \bar{u}_2 \\ \Delta \bar{u}_3 \\ \Delta \bar{e}_1 \\ \Delta \bar{e}_2 \\ \Delta \bar{e}_3 \end{Bmatrix} = \tilde{\mathbf{B}}_s \Delta \mathbf{U} \quad (19)$$

In Eq. (18), $\tilde{\mathbf{B}}_b$ is the bending strain matrix which cooperates the coupling term between the bending strain and displacement, which is different from the formulation by Lee and Kanok-Nukulchai (1998). The additional terms in the two first columns of $\tilde{\mathbf{B}}_b$ reflect the contributions of warping problem shown in the numerical examples 1.

The present strain-displacement $\tilde{\mathbf{B}}$ matrix may be derived from the assumed displacement field using the above definition.

$$\begin{Bmatrix} \Delta^L \tilde{E}_m \\ \Delta^L \tilde{E}_b \\ \Delta^L \tilde{E}_s \end{Bmatrix}_{8 \times 1} = \begin{bmatrix} \tilde{\mathbf{B}}_m & 0 \\ \xi_3 \tilde{\mathbf{B}}_{b1} & \xi_3 \tilde{\mathbf{B}}_{b2} \\ \tilde{\mathbf{B}}_{s1} & \tilde{\mathbf{B}}_{s2} \end{bmatrix}_{8 \times 6} \begin{Bmatrix} \Delta \bar{u} \\ \Delta \boldsymbol{\theta} \end{Bmatrix}_{6 \times 1} \quad (20)$$

In order to remove the locking behaviour, the assumed natural strains described in the following section have been derived and a new $\tilde{\mathbf{B}}_{AS}$ matrix has been implemented instead of using the standard $\tilde{\mathbf{B}}$ matrix.

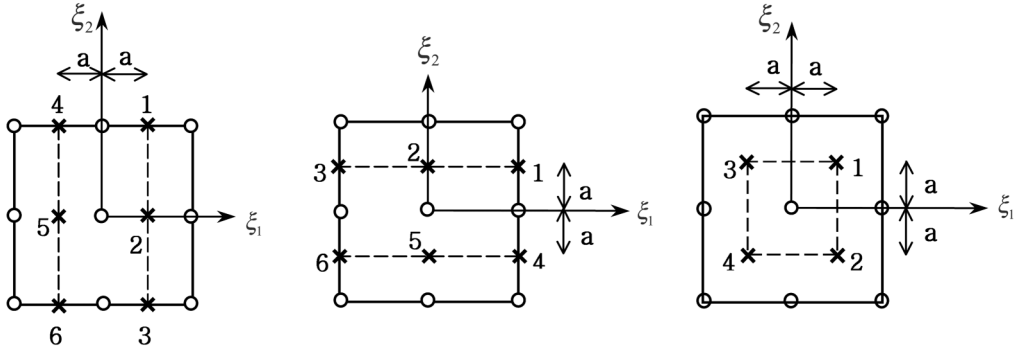


Fig. 4 Sampling points for assumed strains of \tilde{e}_{11} , \tilde{e}_{13} , \tilde{e}_{22} , \tilde{e}_{23} and \tilde{e}_{12}

4. Transverse shear and membrane locking

In order to avoid locking problems, the assumed natural strain method in the 8-node shell element by Kim *et al.* (2003) is used to the 9-node composite shell element. Thus the transverse shear and membrane strain fields are interpolated with the following sampling points in Fig. 4.

The interpolation function for assumed natural strain is shown in the following Table 1.

For assumed membrane strains \tilde{e}_{11} , \tilde{e}_{22} and assumed transverse shear strain \tilde{e}_{13} , \tilde{e}_{23} the following sampling points are used as shown in Fig. 4:

$$\begin{aligned} \tilde{e}_{13}, \tilde{e}_{11} &>> (1/\sqrt{3}, 1)_1 : (1/\sqrt{3}, 0)_2 : (1/\sqrt{3}, -1)_3 : (-1/\sqrt{3}, 1)_4 : (-1/\sqrt{3}, 0)_5 : (-1/\sqrt{3}, -1)_6 \\ \tilde{e}_{23}, \tilde{e}_{22} &>> (1, 1/\sqrt{3})_1 : (0, 1/\sqrt{3})_2 : (-1, 1/\sqrt{3})_3 : (1, -1/\sqrt{3})_4 : (0, -1/\sqrt{3})_5 : (-1, -1/\sqrt{3})_6 \end{aligned} \quad (21)$$

On the other hand, the standard 2×2 Gauss-Legendre numerical integration points are used as sampling points of the assumed membrane shear strain \tilde{e}_{12} . Using these three kinds of sampling points, we can establish assumed strains as

$$\tilde{e}_{13} = \tilde{H}^1 \tilde{E}_{13}^\delta, \quad \tilde{e}_{23} = \tilde{H}^2 \tilde{E}_{23}^\delta, \quad \tilde{e}_{12} = \tilde{H}^3 \tilde{E}_{12}^\delta \quad (22)$$

Table 1 Interpolation function for assumed natural strain fields

| i | \tilde{H}^i | $*P_i(\xi_1)$ | $*Q_i(\xi_2)$ |
|-----|---|---|--|
| 1 | $\sum_{i=1}^2 \sum_{j=1}^3 P_i(\xi_1) Q_j(\xi_2)$ | $P_1(\xi_1) = \frac{1}{2}(1 + \sqrt{3}\xi_1)$ | $Q_1(\xi_2) = \frac{1}{2}\xi_2(\xi_2 + 1)$ |
| 2 | $\sum_{i=1}^2 \sum_{j=1}^3 P_i(\xi_2) Q_j(\xi_1)$ | $P_2(\xi_1) = \frac{1}{2}(1 - \sqrt{3}\xi_1)$ | $Q_2(\xi_2) = 1 - \xi_2^2$ |
| 3 | $\sum_{i=1}^2 \sum_{j=1}^3 P_i(\xi_1) P_j(\xi_2)$ | - | $Q_3(\xi_2) = \frac{1}{2}\xi_2(\xi_2 - 1)$ |

* $P(\xi_2)$ and $Q(\xi_1)$ can be obtained by changing variables.

in which $\delta = 3(i-1) + j$ denotes the position of the sampling point as shown in Fig. 3. The remaining terms in Eq. (22) are given in Table 1. The assumed strain $\tilde{e}_{11}, \tilde{e}_{22}$ have the same interpolation scheme as $\tilde{e}_{13}, \tilde{e}_{23}$, respectively.

5. Constitutive equation

Since the present formulation is based on the natural co-ordinate reference frame, we have introduced here an explicit transformation scheme between natural co-ordinates and the global co-ordinate system, to obtain a constitutive equation based on the natural co-ordinate system.

$$\tilde{\mathbf{S}} = \tilde{J}_0 \tilde{\mathbf{T}} \tilde{\mathbf{D}} \tilde{\mathbf{T}}^T \tilde{\mathbf{E}} = \tilde{\mathbf{C}} \tilde{\mathbf{E}} \quad (23)$$

where \tilde{J}_0 is the determinant of the Jacobian matrix. The constitutive matrix for orthotropic materials with the material angle θ , $\tilde{\mathbf{D}}$ is given by

$$\tilde{\mathbf{D}} = \mathbf{T}_1 \mathbf{C} \mathbf{T}_1^T \quad (24)$$

where \mathbf{C} , \mathbf{T}_1 and $\tilde{\mathbf{D}}$ are obtained straightforwardly.

The transformation matrix \mathbf{T} is given as

$$\mathbf{T} = \begin{bmatrix} \chi_{11}\chi_{11} & \chi_{21}\chi_{21} & \chi_{31}\chi_{31} & 2\chi_{11}\chi_{21} & 2\chi_{21}\chi_{31} & 2\chi_{11}\chi_{31} \\ \chi_{12}\chi_{12} & \chi_{22}\chi_{22} & \chi_{32}\chi_{32} & 2\chi_{12}\chi_{22} & 2\chi_{22}\chi_{32} & 2\chi_{12}\chi_{32} \\ \chi_{13}\chi_{13} & \chi_{23}\chi_{23} & \chi_{33}\chi_{33} & 2\chi_{13}\chi_{23} & 2\chi_{23}\chi_{33} & 2\chi_{13}\chi_{33} \\ \chi_{11}\chi_{12} & \chi_{21}\chi_{22} & \chi_{31}\chi_{32} & \chi_{11}\chi_{22} + \chi_{12}\chi_{21} & \chi_{21}\chi_{32} + \chi_{22}\chi_{31} & \chi_{11}\chi_{32} + \chi_{12}\chi_{31} \\ \chi_{12}\chi_{13} & \chi_{22}\chi_{23} & \chi_{32}\chi_{33} & \chi_{12}\chi_{23} + \chi_{13}\chi_{22} & \chi_{22}\chi_{33} + \chi_{23}\chi_{32} & \chi_{12}\chi_{33} + \chi_{13}\chi_{32} \\ \chi_{11}\chi_{13} & \chi_{21}\chi_{23} & \chi_{31}\chi_{33} & \chi_{11}\chi_{23} + \chi_{13}\chi_{21} & \chi_{21}\chi_{33} + \chi_{23}\chi_{31} & \chi_{11}\chi_{33} + \chi_{13}\chi_{31} \end{bmatrix} \quad (25)$$

where

$$\chi_{ij} = \frac{\partial \xi_j}{\partial X_i} \quad (26)$$

In the case of composite materials, there is a need to adequately define the effective transverse shear stiffness for a wide range of material properties. The effective transverse shear stiffness is obtained by summing the transverse shear stiffness of each layer in the laminate. From the integration of the transverse shear stresses through the laminate thickness,

$$\mathbf{Q} = k_s \sum_{k=1}^N D_{ij}^k (\xi_3^k - \xi_3^{k-1}) \tilde{E}^s = k_s \mathbf{G} \tilde{E}^s \quad \text{for } i, j = 4, 5 \quad (27)$$

The shear stiffness obtained in this method is too large to deal with the real response of the transverse shear energy. Reissner's value of 5/6 may be used as the transverse shear correction factor (k_s) in Eq. (27). Rolfes and Rohwer (1997) proposed an approach based on equilibrium

conditions that result in the real transverse shear stiffness. The formulation considers the actual stacking sequence and more realistic stress distributions. The basic idea is to derive the transverse shear stresses for each layer by integrating the equilibrium equations. Simplification may be done for the integration by assuming two cylindrical bending modes. Having obtained an expression for the transverse shear stresses, the effective transverse shear stiffness is obtained by using the complementary energy density.

The transverse shear stresses, solved using the equilibrium forces in the ξ_1 and ξ_2 directions, are

$$\tilde{S}_3 = \begin{Bmatrix} \tilde{S}_{13} \\ \tilde{S}_{23} \end{Bmatrix}^k = -\int \begin{pmatrix} \tilde{S}_{11, \xi_1}^k + \tilde{S}_{12, \xi_2}^k \\ \tilde{S}_{22, \xi_2}^k + \tilde{S}_{12, \xi_1}^k \end{pmatrix} d\xi_3 \quad (28)$$

The reduced stiffness matrix \bar{Q}_{ij} in of the layer (k) is separated as

$$\tilde{S}_3 = -\int_{-1}^{+1} \left\{ \begin{bmatrix} \bar{Q}_{11} & \bar{Q}_{12} & \bar{Q}_{16} \\ \bar{Q}_{16} & \bar{Q}_{26} & \bar{Q}_{66} \end{bmatrix}^{(k)} \tilde{E}_{, \xi_1} + \begin{bmatrix} \bar{Q}_{16} & \bar{Q}_{26} & \bar{Q}_{66} \\ \bar{Q}_{12} & \bar{Q}_{22} & \bar{Q}_{26} \end{bmatrix}^{(k)} \tilde{E}_{, \xi_2} \right\} d\xi_3 \quad (29)$$

By using laminate elasticity law and assuming cylindrical bending modes, the strain derivatives can be expressed in terms of moment derivatives, then transverse shear forces. The layer-wise parabolic distribution of the transverse shear forces can be comprised to a 2×2 function matrix.

$$\tilde{S}_3 = \begin{bmatrix} H_{11} & H_{12} \\ H_{21} & H_{22} \end{bmatrix} \begin{bmatrix} Q_{13} \\ Q_{23} \end{bmatrix} \quad \text{or} \quad \tilde{S}_3 = h(z)\mathbf{Q} \quad (30)$$

Then the final effective laminate stiffness matrix can be obtained through the strain transverse shear energy and is expressed as follow:

$$\mathbf{G} = \left[\int_{-1}^{+1} h^T G^{-1} h d\xi_3 \right]^{-1} \quad (31)$$

where G are the transverse shear moduli.

6. Incremental equation of equilibrium

At large strain the generalized Hook's law does not represent an approximate material behaviour description because stress-strain relation is non-linear. In practice Hook's law is only applicable to small strain, which constitutive tensor is constant coefficient. Using small strain assumption, the following incremental equilibrium equation is obtained.

$$\int \delta(\Delta^L \tilde{E})^T \tilde{\mathbf{C}} \Delta^L \tilde{E} dV + \int \mathbf{S}(\Delta^{NL} \tilde{E}) dV = {}^{t+\Delta t} \delta W_{ext} - \int \delta(\Delta^L \tilde{E})^T \mathbf{S} dV \quad (32)$$

where superscript t which is generally used as the current configuration is ignored in the above Eq. (32) and superscript $t + \Delta t$ is the adjust incremented configuration, ${}^{t+\Delta t} \delta W_{ext}$ is the external virtual work in $t + \Delta t$.

7. Element stiffness matrices

The total tangent stiffness comprises the material stiffness and the geometric stiffness. The linear part of the Green strain tensor is used to derive the material stiffness matrix and non-linear part of the Green strain tensor is used to derive the geometric stiffness matrix.

7.1 Material stiffness matrix

If the strain-displacement Eq. (17) - Eq. (19) are substituted into Eq. (32), the linearized element material stiffness matrix (\mathbf{K}_L^e) is obtained.

$$\int \delta(\Delta^L \tilde{E})^T \tilde{C} \Delta^L \tilde{E} dV = \delta \Delta \mathbf{U}^T (\int \tilde{\mathbf{B}}^T \tilde{\mathbf{C}} \tilde{\mathbf{B}} dV) \Delta \mathbf{U} = \delta \Delta \mathbf{U}^T \mathbf{K}_L \Delta \mathbf{U} \quad (33)$$

The element stiffness matrix is analytically integrated through the thickness and for the laminate composite rigidity is integrated over each layer. Finally the element stiffness matrix has 6×6 size on the reference-surface of shell element.

$$[\mathbf{K}_L] = \int \begin{bmatrix} \mathbf{K}_L^{11} & \mathbf{K}_L^{12} \\ \mathbf{K}_L^{21} & \mathbf{K}_L^{22} \end{bmatrix}_{6 \times 6} dA \quad (34)$$

where

$$\begin{aligned} \mathbf{K}_L^{11} &= (\tilde{\mathbf{B}}_m)_{AS} [\mathbf{A}] (\tilde{\mathbf{B}}_m)_{AS} + \tilde{\mathbf{B}}_{b1} [\mathbf{B}] (\tilde{\mathbf{B}}_m)_{AS} + (\tilde{\mathbf{B}}_m)_{AS} [\mathbf{B}] \tilde{\mathbf{B}}_{b1} + \tilde{\mathbf{B}}_{b1} [\mathbf{D}] \tilde{\mathbf{B}}_{b1} + (\tilde{\mathbf{B}}_{s1})_{AS} [\mathbf{G}] (\tilde{\mathbf{B}}_{s1})_{AS} \\ \mathbf{K}_L^{12} &= (\tilde{\mathbf{B}}_m)_{AS} [\mathbf{B}] \tilde{\mathbf{B}}_{b2} + \tilde{\mathbf{B}}_{b1} [\mathbf{D}] \tilde{\mathbf{B}}_{b2} + (\tilde{\mathbf{B}}_{s1})_{AS} [\mathbf{G}] (\tilde{\mathbf{B}}_{s2})_{AS} \\ \mathbf{K}_L^{21} &= \tilde{\mathbf{B}}_{b2} [\mathbf{B}] (\tilde{\mathbf{B}}_m)_{AS} + \tilde{\mathbf{B}}_{b2} [\mathbf{D}] \tilde{\mathbf{B}}_{b1} + (\tilde{\mathbf{B}}_{s2})_{AS} [\mathbf{G}] (\tilde{\mathbf{B}}_{s1})_{AS} \\ \mathbf{K}_L^{22} &= \tilde{\mathbf{B}}_{b2} [\mathbf{D}] (\tilde{\mathbf{B}}_{b2})_{AS} + (\tilde{\mathbf{B}}_{s2})_{AS} [\mathbf{G}] (\tilde{\mathbf{B}}_{s2})_{AS} \end{aligned} \quad (35)$$

7.2 Geometric stiffness matrix

Structures composed of plates and shells are stiff in in-plane deformation but flexible in bending deformations. The following geometric stiffness formulation is developed to incorporate the membrane-bending and transverse shear forces on the reference surface and it can be compared with formulation based on Von-Karman theory suitable for thin plate and shell application. Yoo and Choi (2000) presented the nonlinear analysis of the laminated shell element in the three dimensional space. The following geometric stiffness with the stress resultant form may be computationally more efficient than that with the volume integration in the general laminated shell element.

In order to formulate geometric stiffness matrix accurately, the stress values should be evaluated accurately. The accuracy of the computation of stresses for formulation of geometric stiffness matrix is maintained by obtaining the same interpolated strains in the computation of linear stiffness matrix. The stresses are computed at the integration points based on these strains. Ignoring the second order term ξ_3^2 in Eq. (8), the following relation is obtained.

$$\{ {}^{NL}\tilde{E}_{\alpha\beta} \} = \begin{Bmatrix} {}^{NL}\tilde{E}_{11} \\ {}^{NL}\tilde{E}_{22} \\ 2 {}^{NL}\tilde{E}_{12} \\ 2 {}^{NL}\tilde{E}_{23} \\ 2 {}^{NL}\tilde{E}_{13} \end{Bmatrix} = \frac{1}{2} \begin{bmatrix} \frac{\partial u_I}{\partial \xi_1} & 0 & 0 \\ 0 & \frac{\partial u_I}{\partial \xi_2} & 0 \\ \frac{\partial u_I}{\partial \xi_2} & \frac{\partial u_I}{\partial \xi_1} & 0 \\ 0 & \frac{\partial u_I}{\partial \xi_3} & \frac{\partial u_I}{\partial \xi_2} \\ \frac{\partial u_I}{\partial \xi_3} & 0 & \frac{\partial u_I}{\partial \xi_1} \end{bmatrix} \begin{bmatrix} \frac{\partial u_I}{\partial \xi_1} \\ \frac{\partial u_I}{\partial \xi_2} \\ \frac{\partial u_I}{\partial \xi_3} \end{bmatrix} = \frac{1}{2} \mathbf{Q}\mathbf{\Omega} \quad (36)$$

The each component of displacement gradient can be expressed as follows:

$$\begin{aligned} \frac{\partial u_I}{\partial \xi_1} &= \begin{Bmatrix} \frac{\partial u_1}{\partial \xi_1} \\ \frac{\partial u_2}{\partial \xi_1} \\ \frac{\partial u_3}{\partial \xi_1} \end{Bmatrix} = \begin{Bmatrix} \frac{\partial}{\partial \xi_1} \\ \frac{\partial}{\partial \xi_1} \\ \frac{\partial}{\partial \xi_1} \end{Bmatrix} \begin{Bmatrix} \bar{u}_1 \\ \bar{u}_2 \\ \bar{u}_3 \end{Bmatrix} + \xi_3 \begin{Bmatrix} \frac{\partial}{\partial \xi_1} \\ \frac{\partial}{\partial \xi_1} \\ 0 \end{Bmatrix} \begin{Bmatrix} \bar{e}_1 \\ \bar{e}_2 \\ \bar{e}_3 \end{Bmatrix} \\ &= \tilde{\mathbf{G}}_1 \bar{u}_I + \xi_3 \tilde{\mathbf{G}}_2 \bar{e}_I \end{aligned} \quad (37)$$

Similarly the other terms are as follows:

$$\frac{\partial u_I}{\partial \xi_2} = \tilde{\mathbf{G}}_3 \bar{u}_I + \xi_3 \tilde{\mathbf{G}}_4 \bar{e}_I \quad (38)$$

$$\frac{\partial u_I}{\partial \xi_3} = \tilde{\mathbf{G}}_5 \bar{e}_I \quad (39)$$

The incremental gradient displacement ($\mathbf{\Omega}$) for non-linear part with Eq. (15) is as follow:

$$\Delta \mathbf{\Omega} = \begin{Bmatrix} \frac{\partial \Delta u_1}{\partial \xi_1} \\ \frac{\partial \Delta u_2}{\partial \xi_1} \\ \frac{\partial \Delta u_3}{\partial \xi_1} \end{Bmatrix} = \begin{bmatrix} \tilde{\mathbf{G}}_1 & \xi_3 \tilde{\mathbf{G}}_2 \\ \tilde{\mathbf{G}}_3 & \xi_3 \tilde{\mathbf{G}}_4 \\ \mathbf{0} & \tilde{\mathbf{G}}_5 \end{bmatrix} \begin{Bmatrix} \Delta \bar{u}_I \\ \Delta \bar{e}_I \end{Bmatrix} = \tilde{\mathbf{G}} \begin{Bmatrix} \Delta \bar{u} \\ \Delta \bar{\theta} \end{Bmatrix} = \tilde{\mathbf{G}} \Delta \mathbf{U} \quad (40)$$

Then incremental variation of the non-linear part of Green strain is as follows:

$$\delta(\Delta {}^{NL}\tilde{E}) = \delta \Delta \mathbf{Q} \tilde{\mathbf{G}} \Delta \mathbf{U} \quad (41)$$

Substituting the non-linear part of strain into Eq. (32), the following geometric stiffness matrix is obtained.

$$\int S_{\alpha\beta} \delta(\Delta^{NL} \tilde{E}) dV = \int \delta(\Delta^{NL} \tilde{E})^T S_{\alpha\beta} dV = \int \delta \Delta \mathbf{\Omega}^T \Delta \mathbf{Q}^T S_{\alpha\beta} dV \quad (42)$$

The geometric stiffness matrix in the natural coordinate is analytically integrated through the thickness. By the transformation the natural to the global frame, the element geometric stiffness matrix is obtained on the global frame with 6×6 sub matrix.

$$[\mathbf{K}_G] = \int \begin{bmatrix} \mathbf{K}_G^{11} & \mathbf{K}_G^{12} \\ \mathbf{K}_G^{21} & \mathbf{K}_G^{22} \end{bmatrix}_{6 \times 6} dA \quad (43)$$

where

$$\begin{aligned} \mathbf{K}_G^{11} &= 2 \left(\frac{\tilde{\mathbf{G}}_1 N_{11}}{h} + \frac{\tilde{\mathbf{G}}_3 N_{12}}{h} \right) \tilde{\mathbf{G}}_1 + 2 \left(\frac{\tilde{\mathbf{G}}_1 N_{12}}{h} + \frac{\tilde{\mathbf{G}}_3 N_{22}}{h} \right) \tilde{\mathbf{G}}_3 \\ \mathbf{K}_G^{12} &= \frac{2}{3} \left(\frac{6\tilde{\mathbf{G}}_1 M_{11}}{h^2} + \frac{6\tilde{\mathbf{G}}_3 M_{12}}{h^2} \right) \tilde{\mathbf{G}}_2 + \frac{2}{3} \left(\frac{6\tilde{\mathbf{G}}_1 M_{12}}{h^2} + \frac{6\tilde{\mathbf{G}}_3 M_{22}}{h^2} \right) \tilde{\mathbf{G}}_4 \\ &\quad - \frac{2}{3} \left(\frac{3\tilde{\mathbf{G}}_1 Q_1}{2} + \frac{3\tilde{\mathbf{G}}_3 Q_2}{2} \right) \tilde{\mathbf{G}}_5 + \left(\frac{3\tilde{\mathbf{G}}_1 Q_1}{h} + \frac{3\tilde{\mathbf{G}}_3 Q_2}{h} \right) \tilde{\mathbf{G}}_5 \\ \mathbf{K}_G^{21} &= \frac{2}{3} \left(\frac{6\tilde{\mathbf{G}}_2 M_{11}}{h^2} + \frac{6\tilde{\mathbf{G}}_4 M_{12}}{h^2} - \frac{3\tilde{\mathbf{G}}_5 Q_1}{2} \right) \tilde{\mathbf{G}}_1 + \frac{2}{3} \left(\frac{6\tilde{\mathbf{G}}_2 M_{12}}{h^2} + \frac{6\tilde{\mathbf{G}}_4 M_{22}}{h^2} - \frac{3\tilde{\mathbf{G}}_5 Q_2}{2} \right) \tilde{\mathbf{G}}_3 \\ &\quad + \frac{3\tilde{\mathbf{G}}_5 Q_1 \tilde{\mathbf{G}}_1}{h} + \frac{3\tilde{\mathbf{G}}_5 Q_2 \tilde{\mathbf{G}}_3}{h} \\ \mathbf{K}_G^{22} &= \frac{2}{3} \left(\frac{\tilde{\mathbf{G}}_4 N_{12}}{h} + \frac{\tilde{\mathbf{G}}_2 N_{11}}{h} \right) \tilde{\mathbf{G}}_2 + \frac{2}{3} \left(\frac{\tilde{\mathbf{G}}_4 N_{22}}{h} + \frac{\tilde{\mathbf{G}}_2 N_{12}}{h} \right) \tilde{\mathbf{G}}_4 \end{aligned} \quad (44)$$

8. Numerical examples

Several numerical examples are solved to validate the performance of the shell element in both linear and geometrically nonlinear applications. The isotropic and anisotropic composite materials are used for validation. Since the present study shows complex load-deflection curve, it is necessary to use the arc-length control method (Crisfield 1981) in order to trace the full path of load-deflection. The automatic arc-length procedure (Chaisomphob *et al.* 1988 and Ma *et al.* 1989), which has been implemented in the program XFINAS (2003), is used for tracing equilibrium paths of geometrically nonlinear shells.

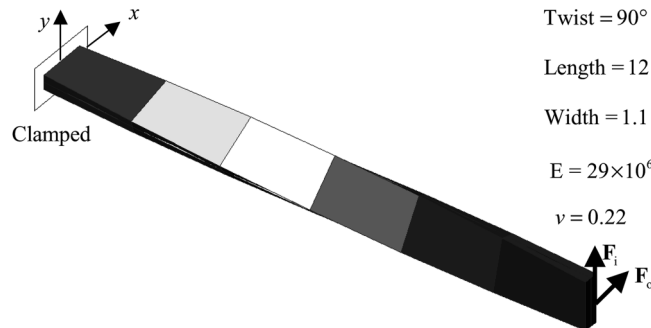


Fig. 5 Twisted beam with 1 × 6 mesh

Table 2 Normalized solutions for twisted beam

| Tip load direction | Formulation | Thickness | | |
|--------------------|---------------------------------|------------|------------|--------------|
| | | $t = 0.32$ | $t = 0.05$ | $t = 0.0032$ |
| In-plane Shear | Lee <i>et al.</i> (1978) | 1.002 | - | 1.013 |
| | Liu <i>et al.</i> (1986) | 1.413 | - | 1.392 |
| | Belytschko <i>et al.</i> (1989) | 0.997 | - | 0.903 |
| | Lee <i>et al.</i> (1998)* | 1.4047 | 1.3691 | 1.3792 |
| | Present | 1.0000 | 1.0000 | 1.0080 |
| Out-of-plane Shear | Lee <i>et al.</i> (1978) | 0.998 | - | 1.002 |
| | Liu <i>et al.</i> (1986) | 1.358 | - | 1.719 |
| | Belytschko <i>et al.</i> (1989) | 0.980 | - | 0.958 |
| | Lee <i>et al.</i> (1998)* | 1.3592 | 1.7027 | 1.7187 |
| | Present | 1.0028 | 1.0029 | 1.0054 |

*Results by Lee and Kanok-Nukulchai are computed independently.

8.1 Twisted beam

Twisted beam suggested by MacNeal and Harder (1985) and has been tested to check the effect of element warping. The in-plane and out-of-plane shear cases are considered for the three type of thickness $t = 0.32, 0.05$ and 0.032 . Observing many elements failed in this test by Belytschko *et al.* (1989), this problem can be considered as a good validation example for general shell elements.

Numerical results shown in Table 2 represent the very good performance of the proposed element. The present element with the kinematic coupling terms improve the warping problem significantly when compared with the element without using the coupling terms by Lee and Kanok-Nukulchai (1998). The absence of the coupling terms caused the error for out-of-plane shears. In this example, it can be pointed out that the resultant shell formulation may need the proper coupling of displacement and bending strain in the twisted beam problem.

8.2 Linear analysis of laminated composite twisted plate

In order to investigate the effects of the coupling term between displacement and bending strain,

Table 3 Deflections by in-plane and out-of-plane shear

| Tip load direction | | 0/90/90/0 | | | 45/-45 | | |
|--------------------|-------------------------|------------|------------|-------------|------------|------------|-------------|
| | | $t = 0.32$ | $t = 0.05$ | $t = 0.032$ | $t = 0.32$ | $t = 0.05$ | $t = 0.032$ |
| Out of plane shear | Solution A | -4576E+02 | -8955E+04 | -3387E+08 | -4582E+02 | -8975E+04 | -3395E+08 |
| | Solution B ^a | -6216E+02 | -1524E+05 | -5802E+08 | -6208E+02 | -1522E+05 | -5795E+08 |
| In plane shear | Solution A | -1425E+03 | -3656E+05 | -1394E+09 | -1412E+03 | -3621E+05 | -1380E+09 |
| | Solution B ^a | -2001E+03 | -5008E+05 | -1908E+09 | -1982E+03 | -4956E+05 | -1888E+09 |

^aResults using Lee and Kanok-Nukulchai theory are computed independently.

the linear analysis of the twisted composite beam with the same geometry in the example 1 is carried out. Material properties used are $E_1 = 3.3 \times 10^3$, $E_2 = E_3 = 1.1 \times 10^3$, $G_{12} = G_{31} = 0.6 \times 10^3$, $G_{13} = 0.44 \times 10^3$ and $\nu = 0.25$. Two lay-ups (0/90/90/0 and 45/-45) are used.

Numerical results are presented in Table 3 for two lay-ups. The present solution with the coupling (Solution A) and without coupling terms (Solution B) are shown in the Table 4. The results without the coupling term show also give errors as same as isotropic cases in the previous example.

8.3 Stress analysis of Z-section plates

The problem in Fig. 6 is used to check the stresses of shell element for problems involving faces and junctions of shell surfaces. Normalized results of stresses at point A and B are presented in Table 4, in comparison with those of White and Abel (1989). With the 8×3 shown in Fig. 6, both elements give very close solutions. Material properties used are $E = 6210$, $\nu = 0.3$ and the thickness $t = 0.1$.

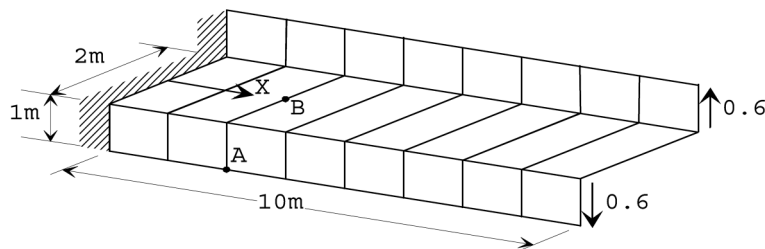


Fig. 6 Z-section plate

Table 4 Normalized stress results for torsion of Z-section plate

Reference solution : $(S_{xx})_A = 108$, $(S_{xx})_B = 36$ (quoted from White and Abel (1989))

| Mesh | $(S_{xx})_A$ | | $(S_{xx})_B$ | |
|--------------|-----------------------|---------|-----------------------|---------|
| | White and Abel (1989) | Present | White and Abel (1989) | Present |
| 4×3 | 1.006 | 1.030 | 1.032 | 1.175 |
| 8×3 | 1.017 | 1.018 | 1.025 | 1.026 |

8.4 Linear analysis of laminated composite plates

In the first example, linear analysis of square laminated plate with three-cross-ply (0/90/0) is carried out. The plate with simple supports is subjected to a uniformly distributed transverse load. The nondimensionalized center deflections are compared with analytical solution by the first order shear deformation theory (FSDT). In the second example, a square laminated plate with angle-ply (45/-45) is analyzed with the same boundary and loading conditions.

Material and geometric properties are

$$E_1 = 25, E_2 = E_3 = 1, G_{12} = G_{31} = 0.5, G_{23} = 0.2, \nu_{12} = \nu_{23} = \nu_{31} = 0.25, a/b = 1$$

From the results in Table 5, the linear solutions of composite laminated square plates are very close to analytical series solutions of first order shear deformation theory.

Table 5 Nondimensionalized center deflections of symmetric cross-ply and anti-symmetric angle-ply plates under uniform load ($\bar{w} = (wh^3 E_2 / q_0 a^4) 10^2, a/b = 1$)

| a/h | (0/90/0) | | (45/-45) | |
|-------|-------------------|---------|-------------------|---------|
| | FSDT ^a | Present | FSDT ^a | Present |
| 4 | 2.6596 | 2.6596 | -- | 2.6035 |
| 10 | 1.0219 | 1.0220 | 1.2792 | 1.2793 |
| 20 | 0.7573 | 0.7573 | 1.0907 | 1.0908 |
| 100 | 0.6697 | 0.6697 | 1.0305 | 1.0306 |

^aSeries solution ($M = 49$) of first-order shear deformation theory (Reddy 1997)

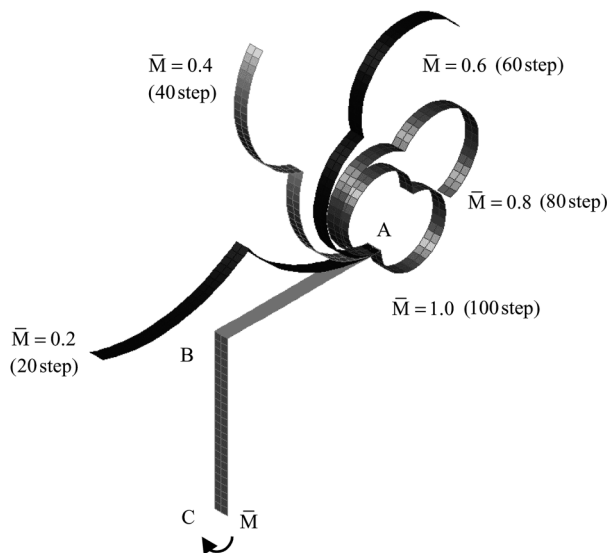


Fig. 7 Progressive deformed shapes corresponding to the increasing loads of Right Angle shell (End A is fixed and End C is free with bending moment)

8.5 Nonlinear analysis of isotropic right angle shell

The right angle shell problem (Simo *et al.* 1993) is shown in Fig. 7 with the sequence of deformed configuration with tip bending moment. The material and geometry property are:

$$E = 1000, \nu = 0.0, t = 1.0, \text{ shell length } L = 120 + 120, \text{ width } b = 10$$

As shown in Fig. 7, the tip bending moment \bar{M} is loaded at the free end. The load parameter of tip bending moment ranges from 0 to $2ML/(3\pi EI)$. One hundred load increment steps are used for the nonlinear solution. The convergence tolerance was set equal to 10^{-4} . All the solutions are converged after 4 iterations. In Fig. 7 the deformed shapes of every 20 load steps are plotted. Complete agreement is found between the present computed results and the elementary beam solution.

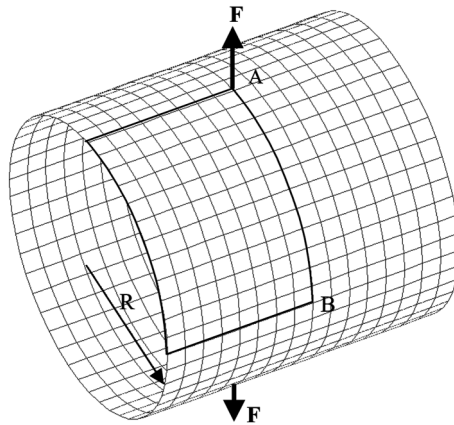


Fig. 8 Pinched cylinder with free edge

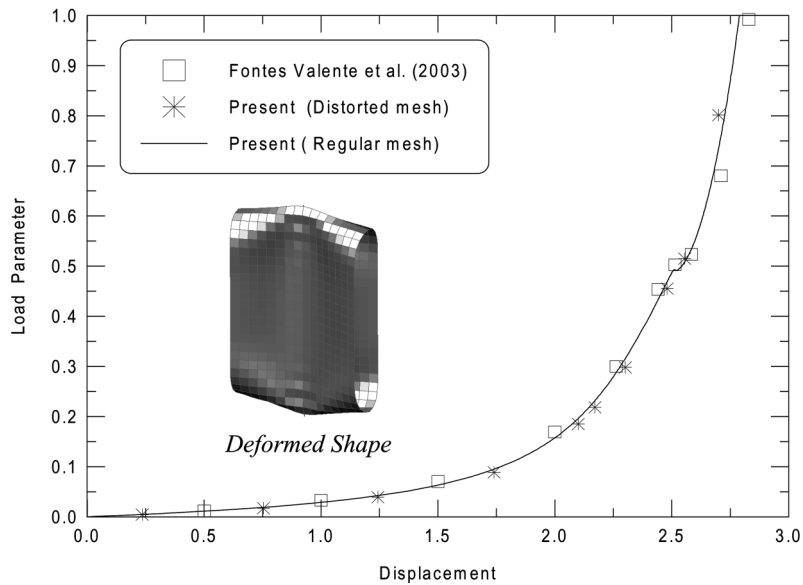


Fig. 9 Load deflection curve of point A of stretched cylinder with free edge

8.6 Nonlinear analysis of isotropic stretched cylinder

The large deformation analysis of a stretched cylinder, as shown in Fig. 8 is carried out with free ends. It is subjected to a pair of concentrated forces. One-octant of the cylinder is analyzed with 6×4 mesh sizes. Additionally, a distorted mesh like Fontes Valente *et al.* (2003) analyzed. Material properties are $E = 10.5 \times 10^6$ and $\nu = 0.3125$. The cylinder length is 10.35, the radius is 4.953 and the thickness is 0.094. The load deflection curve shown in Fig. 9 are compared with Fontes Valente *et al.* (2003). Compared to the references the present results are very good.

8.7 Nonlinear analysis of laminated composite plate

A non-linear analysis of the laminated plate with 16 layers is carried out under uniform load. All boundary edges of the plate are clamped. The plate is subjected to a uniformly distributed load. The entire plate with a 4×4 mesh is used in this analysis.

The material properties used are

$$E_1 = 13.1 \times 10^4 \text{ N/mm}^2; E_2 = E_3 = 1.303 \times 10^4 \text{ N/mm}^2; G_{12} = G_{13} = 0.641 \times 10^4 \text{ N/mm}^2;$$

$$G_{23} = 0.4721 \times 10^4 \text{ N/mm}^2; \nu_{12} = \nu_{23} = \nu_{13} = 0.38$$

Lay-ups $(45^\circ/-45^\circ/0_2^\circ/45^\circ/-45^\circ/90_2^\circ)_s$ (Where the subscript s denotes symmetry.)

The length of the entire square plate is $a = 254$ mm. The total thickness of the laminated is $h = 2.114$ mm and all layers have the same thickness $h/16$.

The nonlinear solutions are obtained by applying 20 equal load incremental step. The result shown in Fig. 10 is compared well with the solution by Saigal *et al.* (1986) and Lee *et al.* (1998). The linear analysis results are compared with Noor and Mothers (1976).

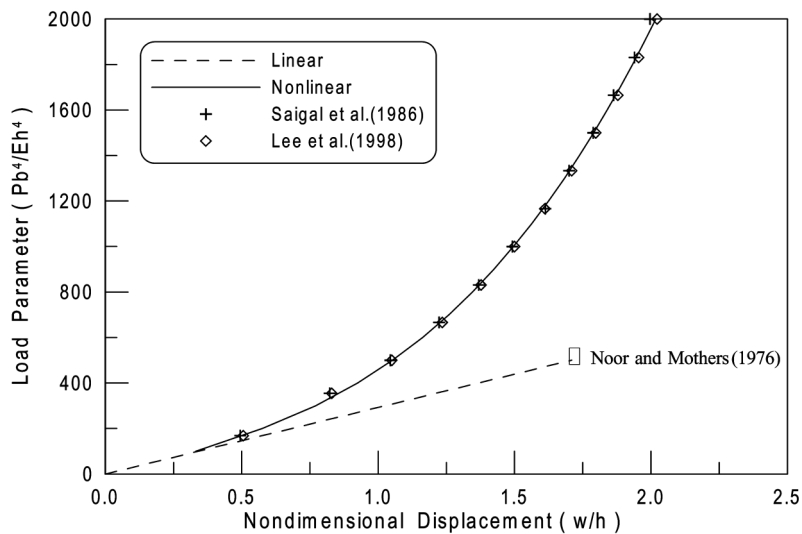


Fig. 10 Load deflection curve of center deflection

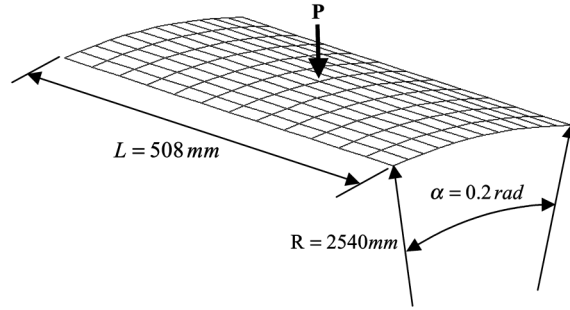


Fig. 11 Geometry of hinged shell

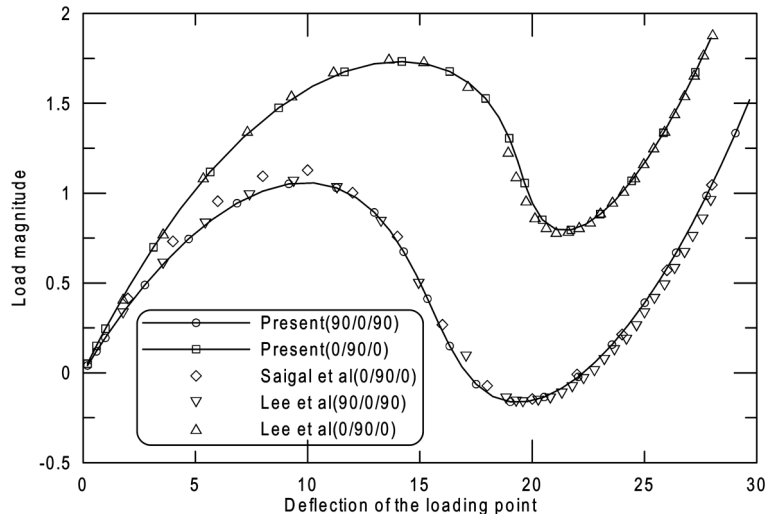


Fig. 12 Displacements of cylindrical shell under point load (12.6 mm)

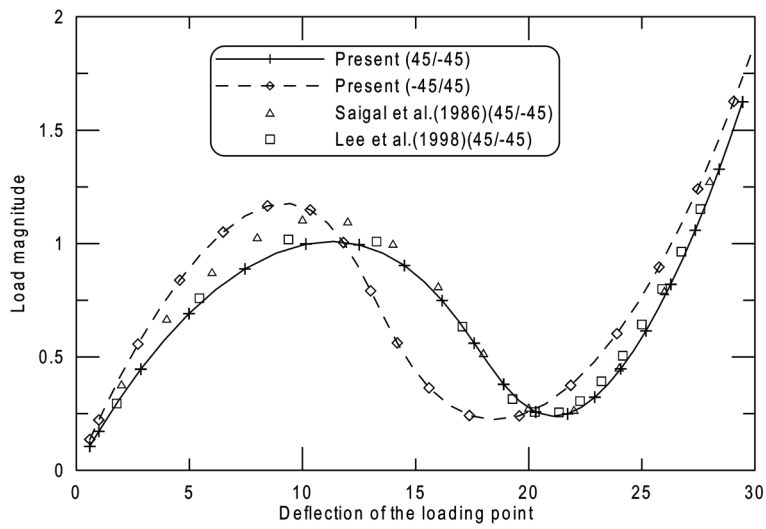


Fig. 13 Displacements of cylindrical shell under point load (12.6 mm)

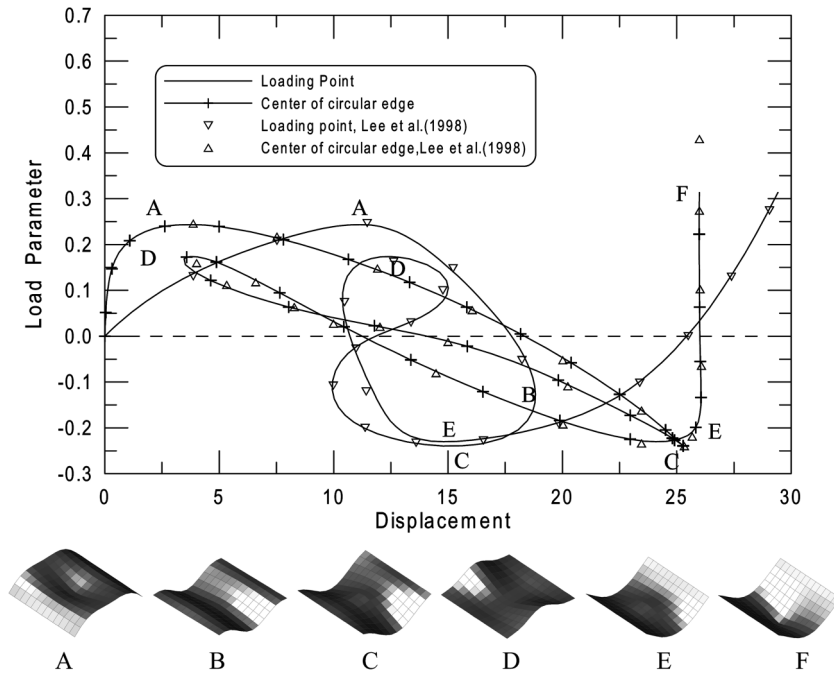


Fig. 14 Displacements of cylindrical shell and deformed shape (symmetric cross-ply (0/90/0), thickness = 6.3 mm)

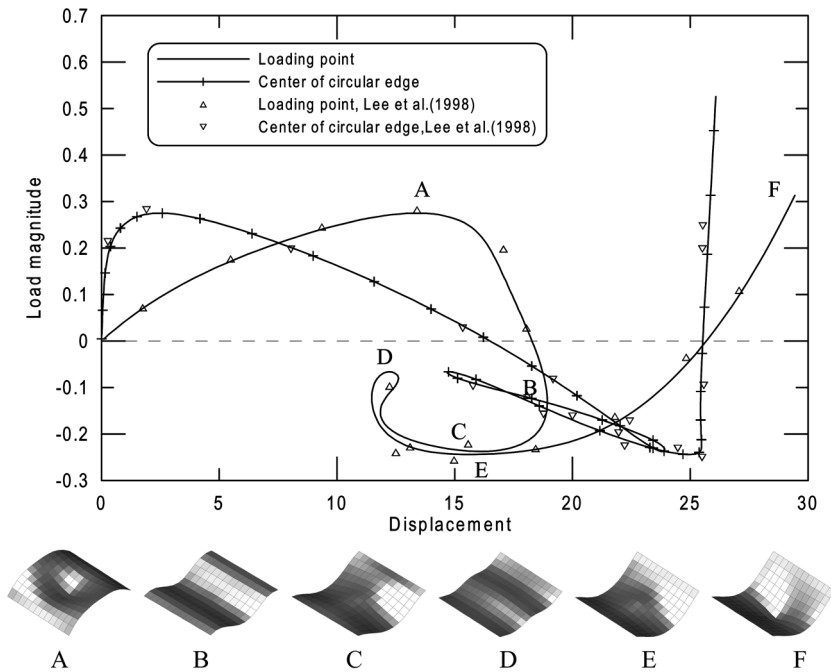


Fig. 15 Displacements of cylindrical shell and deformed shape (antisymmetric angle ply(45/-45), thickness = 6.3 mm)

8.8 Nonlinear analysis of laminated composite shell

The nonlinear analysis of hinged shell is carried out with a 6.3 mm and a 12.6 mm thickness. The quarter model is used for cross ply and the antisymmetric angle ply.

The material properties are Young's modulus $E_1 = 3.3 \text{ kN/mm}^2$, $E_2 = E_3 = 1.1 \text{ kN/mm}^2$, shear modulus $G_{12} = G_{13} = 0.6 \text{ kN/mm}^2$, $G_{23} = 0.44 \text{ kN/mm}^2$, and Poisson's ratio $\nu_{12} = \nu_{13} = \nu_{23} = 0.25$. Lay up used are $0^\circ/90^\circ/0^\circ$ and $90^\circ/0^\circ/90^\circ$.) The other layer up is $45^\circ/-45^\circ$. The geometry of shell is shown in Fig. 11.

In order to investigate the highly nonlinear behaviour, automatic arc-length control method in XFINAS is used. Based on this algorithm, the highly nonlinear equilibrium path are investigated. The Figs. 12 and 13 shows the load-displacements curves for 12.6 mm thickness. The Figs. 14 and 15 show the load-displacements curves for 6.3 mm thickness. The thin shell structure shows more complex load-displacement relationships.

9. Conclusions

In order to demonstrate the capability of the proposed shell element based on the Element-Based Lagrangian Formulation, linear and non-linear problems are discussed above. The Element-Based Lagrangian Formulation makes implementation simpler and easier than the traditional Lagrangian formulations, especially when the assumed natural strain method is involved. The coupling of displacement and bending strain is developed in the present resultant shell element based on Element-Based Lagrangian Formulation. The results showed that the coupling term in the resultant shell element improves a solution significantly in the warping problems. Based on equilibrium approach, an improved transverse shear stiffness considering the actual stacking sequence makes a correction factor no longer required. The present solutions show very good agreement with the analytical solutions and other numerical solutions. Especially, a thin laminated composite shell may be the benchmark test for the large deformation analysis of a laminated composite shell element.

References

- Ahmad, S., Irons, B.M. and Zienkiewicz, O.C. (1970), "Analysis of thick and thin shell structures by curved finite elements", *Int. J. Num. Meth. Eng.*, **2**, 419-451.
- Belytschko, T., Wong, B.L. and Stolarski, H. (1989), "Assumed strain stabilization procedure for the 9-node Lagrange shell element", *Int. J. Num. Meth. Eng.*, **28**, 385-414.
- Chaisomphob, T., Kanok-Nukulchai, W. and Nishino, F. (1988), "An automatic arc length algorithm for tracing equilibrium paths of nonlinear structures", *Proc. of JSCE, Struct. Eng./Earthq. Eng.*, **5**, 205-208.
- Crisfield, M.A. (1981), "A fast incremental/iterative solution procedure that handles snap-through", *Comput. Struct.*, **13**, 55-62.
- Fontes Valente, R.A., Natal Jorge, R.M., Cardoso, R.P.R., Ce'sar de Sa', J.M.A. and Gra'cio, J.J.A. (2003), "On the use of an enhanced transverse shear strain shell element for problems involving large rotations", *Comput. Mech.*, **30**, 286-296.
- Huang, H.C. and Hinton, E. (1986), "A new nine node degenerated shell element with enhanced membrane and shear interpolation", *Int. J. Num. Meth. Eng.*, **22**, 73-92.
- Hughes, T.J.R. and Liu, W.K. (1981), "Nonlinear finite element analysis of shells: Part I. Three-dimensional shells", *Comput. Meth. Appl. Mech. Eng.*, **26**, 331-362.

- Jang, J. and Pinsky, P.M. (1987), "An assumed covariant strain based 9-node shell element", *Int. J. Num. Meth. Eng.*, **24**, 2389-2411.
- Kanok-Nukulchai, W. and Wong, W.K. (1988), "Element-based Lagrangian formulation for large-deformation analysis", *Comput. Struct.*, **30**, 967-974.
- Kim, K.D., Lomboy, G.R. and Han, S.C. (2003), "A co-rotational 8-node assumed strain shell element for postbuckling analysis of laminated composite plates and shells", *Comput. Mech.*, **30**(4), 330-342.
- Kim, K.D. and Park, T.H. (2002), "An 8-node assumed strain element with explicit integration for isotropic and laminated composite shells", *Struct. Eng. Mech.*, **13**(4), 387-410.
- Kim, K.D., Park, T. and Voyiadjis, G.Z. (1998), "Postbuckling analysis of composite panels with imperfection damage", *Comput. Mech.*, **22**, 375-387.
- Kim, K.D. and Voyiadjis, G.Z. (1999), "Non-linear finite element analysis of composite panels", *Composites Part B: Engineering*, **30**(4), 365-381.
- Lee, S.J. and Kanok-Nukulchai, W. (1998), "A nine-node assumed strain finite element for large deformation analysis of laminated shells", *Int. J. Num. Meth. Eng.*, **42**, 777-798.
- Lee, S.W. and Pian, T.H.H. (1978), "Improvement of plate and shell finite elements by mixed formulation", *AIAA J.*, **16**, 29-34.
- Liu, W.K., Lam, D., Law, S.E. and Belytschko, T. (1986), "Resultant stress degenerated shell element", *Comput. Meth. Appl. Mech. Eng.*, **55**, 259-300.
- Ma, H. and Kanok-Nukulchai, W. (1989), "On the application of assumed strained methods", *Structural Engineering and Construction, Achievements, Trends and Challenges*, Kanok-Nukulchai *et al.* (eds.), AIT, Bangkok.
- MacNeal, R.H. (1982), "Derivation of element stiffness matrices by assumed strain distributions", *Nucl. Engng. Design*, **33**, 1049-1058.
- Noor, A.K. and Mathers, M.D. (1976), "Anisotropy and shear deformation in laminated composite plates", *AIAA*, **14**, 282-285.
- Ramm, E. (1977), "A plate/shell element for large deflections and rotations", *Nonlinear Finite Element Analysis in Structural Mechanics*, Wunderlich, W., Stein, E., Bathe, K.J. (eds.), M.I.T. Press, NY.
- Reddy, J.N. (1997), *Mechanics of Laminated Composite Plates*, CRC Press, Florida.
- Rolfes, R. and Rohwer, K. (1997), "Improved transverse shear stress in composite finite element based on first order shear deformation theory", *Int. J. Num. Meth. Eng.*, **40**, 51-60.
- Saigal, S., Kapania, R.K. and Yang, Y.T. (1986), "Geometrically nonlinear finite element analysis of imperfect laminated shells", *J. Compos. Mater.*, **20**, 197-214.
- Simo, J.C. and Hughes, T.J.R. (1986), "On the variational formulations of assumed strain methods", *J. Appl. Mech.*, ASME, **53**, 51-54.
- Simo, J.C. (1993), "On a stress resultant geometrically exact shell model. Part VII: Shell intersections with 5/6-DOF finite element formulations", *Comput. Meth. Appl. Mech. Eng.*, **108**, 319-339.
- White, D.W. and Abel, J.F. (1989), "Testing of shell finite element accuracy and robustness", *Finite Element Method in Analysis and Design*, **6**, 129-151.
- Wong, Wai-Kong (1984), "Pseudo Lagrangian formulation for large deformation analysis of continua and structures", Master Thesis, School of Civil Engineering, A.I.T.
- XFINAS (2003), *Nonlinear Structural Dynamic Analysis System*, School of Civil Engineering, A.I.T., Thailand.
- Yoo, S.W. and Choi, C.K. (2000), "Geometrically nonlinear analysis of laminated composites by an improved degenerated shell element", *Struct. Eng. Mech.*, **9**(1), 123-456.